Time resolution and high-counting rate performance of plastic scintillation counter with multiple MPPC readout

Sekiya, R.; Drozd, V.; Tanaka, Y. K.; Itahashi, K.; Fujioka, H.; Matsumoto, S. Y.; Saito, T. R.; Suzuki, K.

Published in:
Nuclear Instruments and Methods in Physics Research, Section A: Accelerators, Spectrometers, Detectors and Associated Equipment

DOI:
10.1016/j.nima.2022.166745

Publication date:
2022

Nuclear Inst. and Methods in Physics Research, A 1034 (2022) 166745

Contents lists available at ScienceDirect

Nuclear Inst. and Methods in Physics Research, A

journal homepage: www.elsevier.com/locate/nima

Time resolution and high-counting rate performance of plastic scintillation counter with multiple MPPC readout

R. Sekiya [a,b,*], V. Drozd [c,d], Y.K. Tanaka [b], K. Itahashi [b,e], H. Fujioka [f], S.Y. Matsumoto [a,b], T.R. Saito [b,d,g], K. Suzuki [h]

[a] Department of Physics, Kyoto University, Kitashirakawa-Oiwake, Sakyo, Kyoto 606-8502, Japan
[b] Cluster for Pioneering Research, RIKEN, 2-1 Hirosawa, Wako, Saitama 351-0198, Japan
[c] Energy and Sustainability Research Institute Groningen, University of Groningen, Nijenborgh 6, 9747 AG Groningen, The Netherlands
[d] GSI Helmholtzzentrum für Schwerionenforschung GmbH, Planckstraße 1, 64291 Darmstadt, Germany
[e] Nishina Center for Accelerator-Based Science, RIKEN, 2-1 Hirosawa, Wako, Saitama 351-0198, Japan
[f] Department of Physics, Tokyo Institute of Technology, 2-12-1 Ookayama, Meguro, Tokyo 152-8551, Japan
[g] School of Nuclear Science and Technology, Lanzhou University, 222 Shouth Tianshui Road, Lanzhou, Gansu Province, 730000, China
[h] Stefan-Meyer-Institut für subatomare Physik, Boltzmangasse 3, 1090 Vienna, Austria

ARTICLE INFO

Keywords:
SiPM
Timing counter
High counting rate performance

ABSTRACT

We have been developing a plastic scintillation counter for the WASA detector. The performance of a plastic scintillation counter with Multi-Pixel Photon Counter (MPPC) readout has been systematically investigated for minimum ionizing particles in terms of the time resolution and the signal amplitude stability. The performance was evaluated under various incident conditions of 2.5 GeV/c proton beams and with different MPPC settings. A plastic scintillator with a size of $550 \times 38 \times 8$ mm^3 was optically coupled with multiple MPPCs at each plane with a size of 38×8 mm^2 for detecting the scintillation photons. The observed time resolution ranges in 37–80 ps (σ) depending on the incident positions and angles for the case of three MPPCs attached to each end. We found the time resolution and the signal amplitude fairly consistent up to the counting rate of 0.2 MHz.

1. Introduction

Recently Silicon PhotoMultipliers (hereinafter referred to as Multi-Pixel Photon Counters, MPPCs) have been widely used as photon detectors of scintillation counters in high energy and nuclear physics experiments. Besides PhotoMultiplier Tubes (PMTs) commonly adopted, MPPCs have been attracting attention as alternatives for many reasons including the lower cost, the compact design, the smaller power consumption, and the immunity to a magnetic field. MPPCs have a fast timing response so that they can be employed for developing a precise timing counter in combination with fast-timing plastic scintillators [1–7].

We have newly developed a plastic scintillation counter with MPPCs. A set of such counters will be assembled in a form of a cylindrical barrel to form Plastic Scintillator Barrel (PSB) and installed in the WASA detector [8] by replacing the existing scintillation counters. The WASA has been installed at the mid-focal plane of the Fragment Separator [9] at GSI, Germany and will be used for spectroscopy of meson–nucleus bound systems [10] and measurement of hypernuclei [11].

In order to meet experimental requirements, we need to improve the time resolution of the scintillation counters to achieve better integration with other detectors under high counting rate conditions. The new PSB is located to cover a large solid angle in view of the reaction target and is used for identification of charged decay particles from the nuclear reactions by measuring the energy loss and timing information. The PSB consists of 46 slats of plastic scintillation counters with a size of $550 \times 38 \times 8$ mm^3 and each plastic scintillator is read by multiple MPPCs at the both ends as schematically shown in Fig. 1. The PSB is aiming at stable operation with a time resolution better than 100 ps (σ) under a typical counting rate of 10 MHz, namely ∼ 200 kHz per slat, in a magnetic field of ∼1 T.

We have made systematic investigation of a single slat of the PSB performance by changing the configurations such as the number of the MPPCs, applied bias voltage, and hit positions and angles of the charged particles. We have evaluated the stability of the signal amplitude and the time resolution at very high counting rates up to 5 MHz. The measurement was conducted with 2.5 GeV/c proton beams at the Cooler Synchrotron (COSY), Jülich. In this paper, we report the measurement in Section 2, the analysis in Section 3, and the results and discussions on the measured performance in Section 4.

* Corresponding author at: Department of Physics, Kyoto University, Kitashirakawa-Oiwake, Sakyo, Kyoto 606-8502, Japan.
E-mail address: sekiya.ryohei.64r@st.kyoto-u.ac.jp (R. Sekiya).

https://doi.org/10.1016/j.nima.2022.166745
Received 2 August 2021; Received in revised form 3 April 2022; Accepted 3 April 2022
Available online 18 April 2022

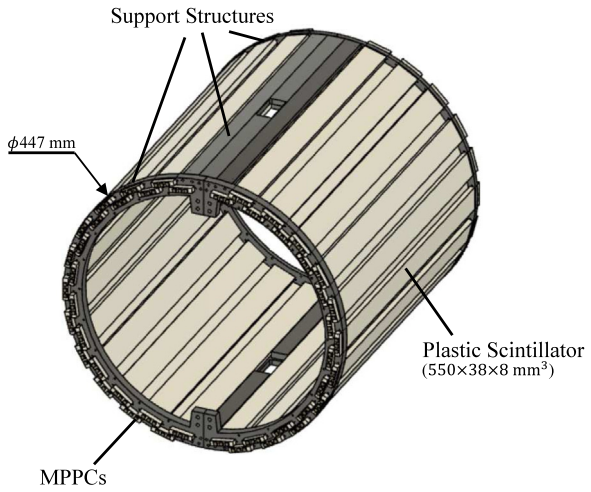

Fig. 1. A full view of the PSB consisting of 46 plastic scintillation counters with a size of $550 \times 38 \times 8$ mm^3. The outer plastics and the inner plastics are arranged with a diameter of 463.5 mm and 442.0 mm, respectively. In the scheme, 3 MPPCs are attached to each end of the plastic scintillators.

2. Measurement

2.1. Experimental setup

Fig. 2 depicts a schematic setup of the measurement in COSY-TOF beamline. We made use of 2.5 GeV/c proton beam with the intensity ranging from 5 kHz to 5 MHz extracted from the synchrotron by a spill length of ∼110 s. The beam spot size was estimated to be 25 mm (H) and 13 mm (V). We placed two identical scintillation counters, PSB1 and PSB2, perpendicular to the incident proton beams and mounted them on a movable stage in the x-direction. As the plastic scintillator, we adopted Eljen Technology EJ-230 with a refractive index of 1.58, an attenuation length of 120 cm and rise and decay time of 0.5 ns and 1.5 ns, respectively. The size is $550 \times 38 \times 8$ mm^3. We used S13360-6050CS manufactured by Hamamatsu Photonics for the MPPCs [12] and directly attached them to each plane with a size of 38×8 mm^2 of the scintillator by an optical grease TSK5353 (Momentive Performance Materials). The effective photosensitive area of a single MPPC is 6×6 mm^2 and has 14400 pixels with a pitch of 50 μm. The breakdown voltage in the specifications is ∼51.5 V [12]. We connected the MPPCs on the same PSB end in series and the electrically summed signal was amplified by the amplifiers that had been developed in Ref. [1]. Bias voltages to the MPPCs were applied by using a power supply DT1470ET (CAEN). In the downstream of PSB2, we placed four small plastic scintillators, Finger1 in the vertical direction with a size of 3×3×45 mm^3 and Finger2-1, 2-2, and 2-3 in the horizontal direction with a size of 3×3×30 mm^3 at y = 16, 8 and 0 mm, respectively, as reference counters attached to Hamamatsu H3171-04 PMTs.

Signals from the detectors were recorded by using a waveform digitizer CAEN V1742, which measures input waveform with a maximum sampling frequency of 5 GHz, an input dynamic range of 1 V peak to peak and 12 bit resolution, operated at a sampling rate of 2.5 GHz to analyze the timing information and the amplitude of the signals. The data acquisition deadtime was negligible in the present application. Counting rates were monitored with GSI VUPROM2 (100 MHz scaler) [13]. The data acquisition system was triggered by the coincidence of the top and bottom PMTs of Finger1. The recorded data were analyzed as explained in Section 2.2.

We have conducted systematic measurements to study the performance of the detector by setting various configurations for hit positions (x_p) and incident angles (θ_p) of the proton beams, number of MPPCs per end (N_{MPPC}), applied bias voltages (V_{bias}), and the beam intensity on the PSBs (I_p). The hit position x_p is measured from the center of the PSBs and the angle θ_p is the incident angle with respect to the normal vector of the PSBs. We changed x_p to cover a whole region of the PSBs in a range between −24 cm to +24 cm. We rotated the PSBs around the vertical axis y by $\theta_p = 0°$, 30°, 60° and 70°. We employed N_{MPPC} of 1, 2, 3, and 4 and changed the bias voltage per MPPC ($V_{\mathrm{bias}}/N_{\mathrm{MPPC}}$) between 54 V and 58 V. We took data with I_p between 5 kHz and 5 MHz.

2.2. Analysis

Fig. 3 (top) shows typical waveform data of PSB2 (left) recorded by the waveform digitizer, where 2 MPPCs were attached to each end with $V_{\mathrm{bias}}/N_{\mathrm{MPPC}} = 57$ V. The hit timing of the signal was analyzed to suppress the time-walk by employing a method of a constant-fraction discriminator [14]. We have realized the method by a software choosing the delay and fraction parameters to be $t_d = 3.2$ ns and $f = 0.15$, respectively (see Ref. [15] for details). The amplitude of the signal with respect to the baseline was obtained by quadratically fitting five consecutive points of the waveform around its minimum point, as displayed by the red curve.

The time resolutions of the PSBs were evaluated from measured time-of-flight (TOF) distributions between PSB1 and PSB2 ($T_1 - T_2$), PSB1 and Finger1 ($T_1 - T_{\mathrm{F}}$), and PSB2 and Finger1 ($T_2 - T_{\mathrm{F}}$), where T_1, T_2, and T_{F} denote the hit timing at PSB1, PSB2, and Finger1, respectively. T_1 and T_2 were averages of the hit timing obtained with the left and right MPPCs, and T_{F} was an average of the top and bottom PMTs. The three TOF histograms were fitted with Gaussian functions to evaluate the standard deviations, $\sigma(T_1 - T_2)$, $\sigma(T_1 - T_{\mathrm{F}})$, and $\sigma(T_2 - T_{\mathrm{F}})$. The time resolutions of PSB1 (σ_1), PSB2 (σ_2) and Finger1 (σ_{F}) were calculated using the measured quantities by an equation

$$\begin{pmatrix} \sigma_1^2 \\ \sigma_2^2 \\ \sigma_{\mathrm{F}}^2 \end{pmatrix} = \frac{1}{2} \begin{pmatrix} 1 & -1 & 1 \\ 1 & 1 & -1 \\ -1 & 1 & 1 \end{pmatrix} \begin{pmatrix} \sigma(T_1 - T_2)^2 \\ \sigma(T_2 - T_{\mathrm{F}})^2 \\ \sigma(T_1 - T_{\mathrm{F}})^2 \end{pmatrix} \quad (1)$$

obtained after solving simultaneous equations. The time resolution of Finger1 was evaluated to be 118 ps by taking an average of the data with $I_p < 100$ kHz.

Fig. 3 (bottom) shows a distribution of amplitudes measured by PSB2 (left) with $N_{\mathrm{MPPC}} = 2$ and $V_{\mathrm{bias}}/N_{\mathrm{MPPC}} = 57$ V. The distribution exhibits an asymmetric peak (around 100 mV), which can be fitted by an empirical function of the abscissa x in a form of $a_0 \exp(-(x - a_1)^2/(a_2 + a_3 x)^2)$, as displayed by the red curve. We adopted the most probable value $A_{\mathrm{mpv}} = a_1$ and the full width at half maximum (FWHM) value W of the fitted function as the representative amplitude and spread, respectively.

To estimate I_p over a very wide dynamic range of 5 kHz to 5 MHz, we employed two methods. As for the first method, we directly measure I_p by the counting rates of the PSBs. This is accurate for relatively low intensities. For higher intensities > 100 kHz, this method is potentially biased because of the too high counting rate. The second method utilizes Finger1 counting rates since the counting rate by the Finger1 stays low even for the maximum beam intensity. The beam profile is relatively stable and a fraction of the beam measured by the Finger1 stays nearly constant during the measurements. Finger1 and PSB counting rates are linearly correlated and we calibrate the Finger1 counting rate with the PSB counting rate at a range of $I_p < 100$ kHz as shown in Fig. 4 (top). For higher intensities $I_p > 100$ kHz, we estimated I_p by the calibrated Finger1 counting rate since the PSB counting rate is saturated as shown in Fig. 4 (bottom).

As shown in Fig. 5, there are many fine spikes in a spill due to micro structure of the extracted beam. We selected the events in which the beam intensity was relatively stable for a certain period of time. We selected points where the neighboring intensities are within ± 30%.

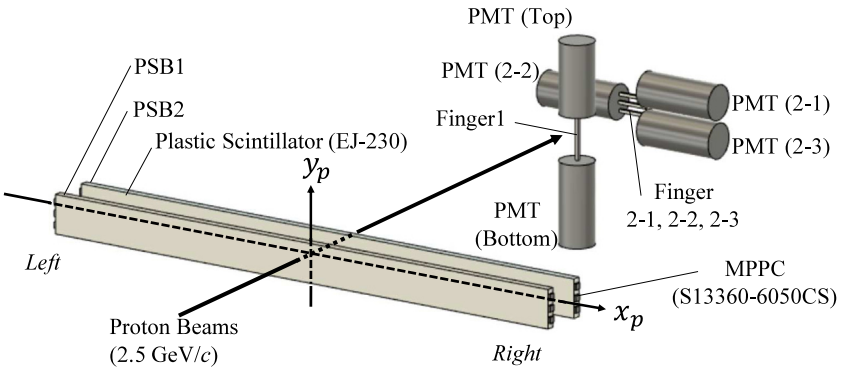

Fig. 2. A schematic view of the experimental setup.

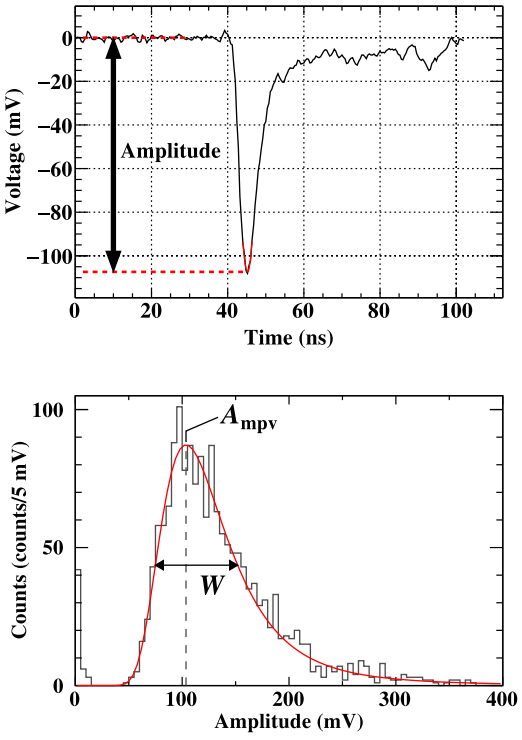

Fig. 3. Top: A typical waveform of PSB2 (left) with $N_{\mathrm{MPPC}} = 2, V_{\mathrm{bias}}/N_{\mathrm{MPPC}} = 57$ V obtained by the waveform digitizer with a sampling rate of 2.5 GHz. The red curve shows a fitted quadratic function around the minimum point to determine the amplitude. Bottom: amplitude distribution of PSB2 (left) with $N_{\mathrm{MPPC}} = 2, V_{\mathrm{bias}}/N_{\mathrm{MPPC}} = 57$ V. The red curve shows a fit function $a_0 \exp(-(x-a_1)^2/(a_2+a_3x)^2)$.

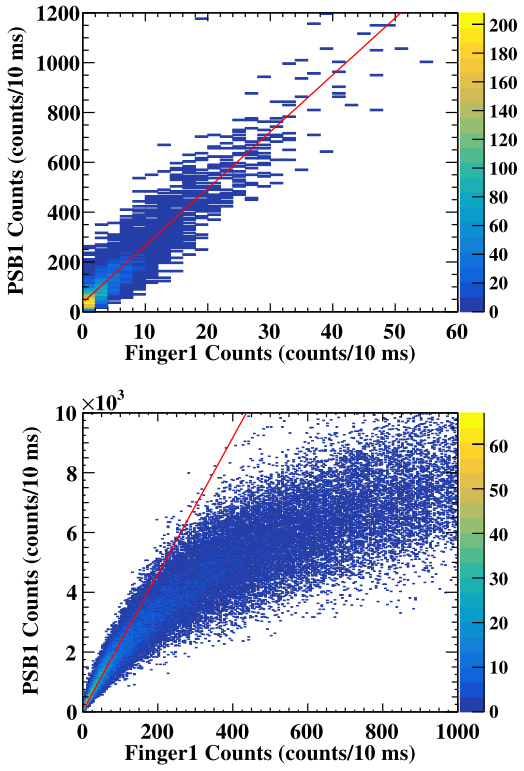

Fig. 4. Top: Correlation between the integrated counts for 10 ms by PSB1 and by Finger1. The fit result with a linear function is denoted by the red line. Bottom: The same correlation under higher intensities.

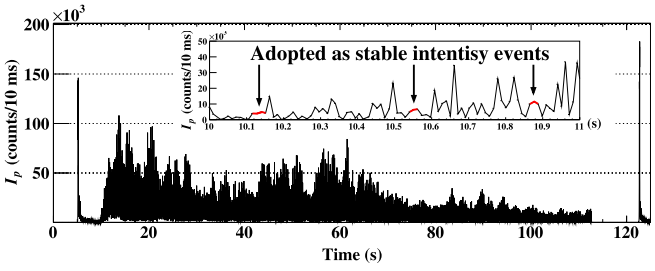

Fig. 5. A typical time structure of the beam. The ordinate corresponds to the number of counts of PSB1 integrated in 10 ms and the abscissa to the time measured by the 100 kHz clock generator. The interval of the neighboring points is nearly 10 ms. The figure expanded from 10 s to 11 s is also shown.

3. Results and discussions

Fig. 6 (top) depicts measured hit-position (x_p) dependence of the time resolution of the PSB1 with 3 MPPCs attached to each end applying different bias voltages per MPPC ($V_{\mathrm{bias}}/N_{\mathrm{MPPC}}$) from 55 to 58 V. We find a good resolution ranging in 55–80 ps over the whole measured region. Better resolution is achieved with higher $V_{\mathrm{bias}}/N_{\mathrm{MPPC}}$. The measured dependence shows the best resolution near the center of the slat $x_p \sim 0$ with $V_{\mathrm{bias}}/N_{\mathrm{MPPC}} = 57$ or 58 V. In a similar analysis of the data taken with selecting different y positions by Fingers 2-1, 2-2, and 2-3, we find that the time resolution does not significantly depend on the hit positions in the y direction.

In order to investigate the position dependence, the resolutions evaluated for the left and right MPPCs alone are shown in Fig. 6 (bottom). The time resolution shows a clear dependence on the distance to the hit positions from the MPPCs for both left and right MPPCs in a comparable way. The dependence is understood in terms of the solid angle of the MPPC viewed from each hit position, the light attenuation,

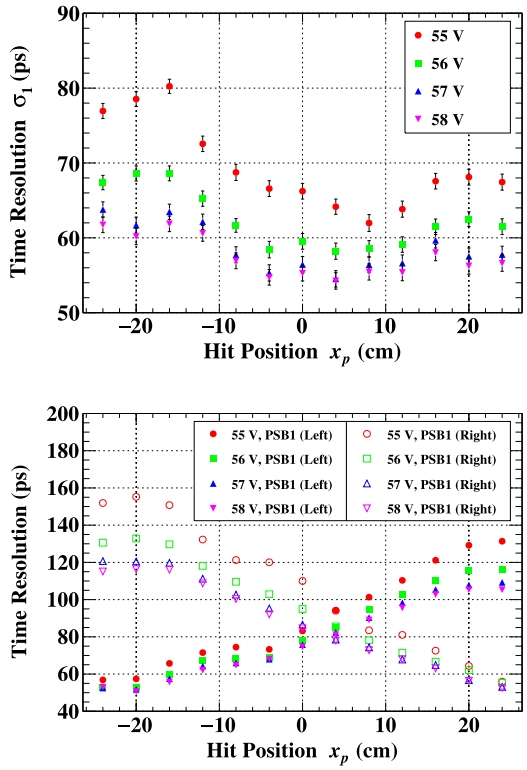

Fig. 6. Top : The position dependence of the time resolution σ_1 with $N_{\mathrm{MPPC}} = 3$. Bottom : The position dependence of the time resolution for left or right MPPCs on PSB1. Where not visible, the errors are within the symbol size.

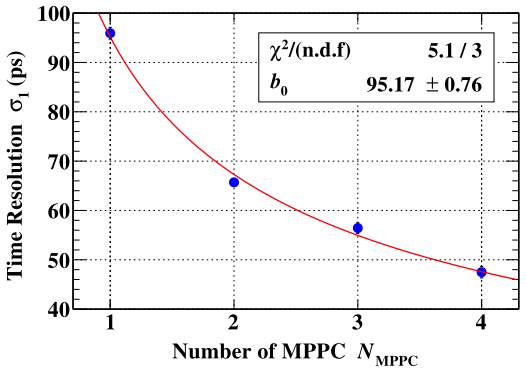

Fig. 7. N_{MPPC} dependence of the time resolution σ_1 at $x_p = 0$ cm. The MPPCs were operated at $V_{\mathrm{bias}}/N_{\mathrm{MPPC}} = 57$ V. A fit with $b_0/\sqrt{N_{\mathrm{MPPC}}}$ is displayed by the red curve.

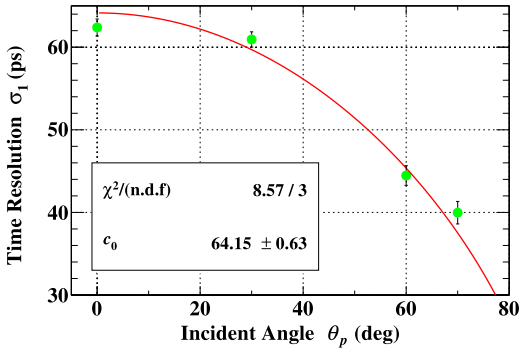

Fig. 8. The incident angle θ_p dependence of the time resolution σ_1 at $x_p = 0$ cm with 3 MPPCs operated at $V_{\mathrm{bias}}/N_{\mathrm{MPPC}} = 56$ V. The red curve shows a fit with $c_0\sqrt{\cos\theta_p}$.

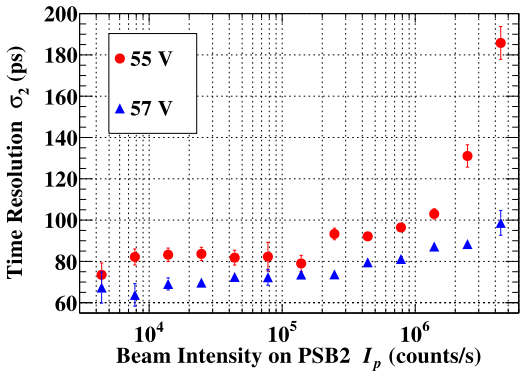

Fig. 9. The intensity dependence of the time resolution with $V_{\mathrm{bias}}/N_{\mathrm{MPPC}} = 55$ V and 57 V. Two MPPCs were used for both ends of the plastic scintillators.

and the path length spread. The time resolution is nearly symmetric for the left and right MPPCs with respect to $x_p = 0$ cm. A slight deviation is observed for the uneven quality of the MPPCs. The hit-position dependence of the resolution of the PSB1 shown in Fig. 6 (top) is explained well by the dependence in Fig. 6 (bottom). In the analysis of the PSB2 data, we find similar results.

We measured the time resolution changing with N_{MPPC}. Fig. 7 shows the N_{MPPC} dependence of the time resolution for $V_{\mathrm{bias}}/N_{\mathrm{MPPC}} = 57$ V with the hit position $x_p = 0$. We achieve the best time resolution of ~50 ps for $N_{\mathrm{MPPC}} = 4$. We observe σ_1 nearly inversely proportional to the square root of the N_{MPPC} as expected. We have made a chi-square fit of the data with a function $b_0/\sqrt{N_{\mathrm{MPPC}}}$ using a parameter b_0 and obtained $\chi^2/(\mathrm{n.d.f.}) = 5.1/3$, where n.d.f. denotes the number of degrees of freedom. The obtained b_0 is 95.17 ± 0.76 ps, which corresponds to the time resolution in case of $N_{\mathrm{MPPC}} = 1$.

Fig. 8 shows the incident-angle θ_p dependence of σ_1. We obtain smaller σ_1 with larger θ_p due to the larger energy loss ΔE of protons crossing the counter. The σ_1 is nearly inversely proportional to $\sqrt{\Delta E}$. We have made a chi-square fit of the data with a function $c_0\sqrt{\cos\theta_p}$ using a parameter c_0, which indicates the time resolution for $\theta_p = 0$ degrees. The fit result is shown by the red curve for $V_{\mathrm{bias}}/N_{\mathrm{MPPC}} = 56$ V. Although the position distribution of the beam in the scintillator is broader for larger θ_p, the resultant effects due to the larger spot size are not clearly observed and are negligible.

Performance of the PSB under extremely high rate conditions is important for high-luminosity experiments. Due to the intensity fluctuation of the incident beam during measurement, we estimated instantaneous intensities I_p based on the counting rates of the Finger1 as described in Section 2.1. In the following analysis, we employed the data of the PSB2 with N_{MPPC}=2.

Fig. 9 shows the time resolution as a function of I_p. Up to $I_p \sim 1$ MHz, σ_2 slightly increases for both $V_{\mathrm{bias}}/N_{\mathrm{MPPC}} = 55$ V and 57 V. For $I_p > 1$ MHz, we observe a steep rise in the case of $V_{\mathrm{bias}}/N_{\mathrm{MPPC}} = 55$ V and a slight increase in the case of 57 V.

The intensity dependence of the time resolution can be partly understood in terms of the amplitude of the signals. Fig. 10 shows the I_p dependence of the signal amplitude A_{mpv} and width W normalized by A_{mpv}. The latter directly contributes to the relative resolution of the energy loss of particles. We find A_{mpv} is relatively stable up to 300 kHz, slowly drops for higher I_p and reaches 70% reduction at 4 MHz compared with those at ~10 kHz. This may have caused deterioration of the time resolution. Ratio of the width to the amplitude W/A_{mpv} is also relatively stable up to 100 kHz and slowly rises for higher I_p as shown in Fig. 10 (bottom).

While investigating the reason for the amplitude reduction and relative width broadening, we observed fluctuations of the applied bias

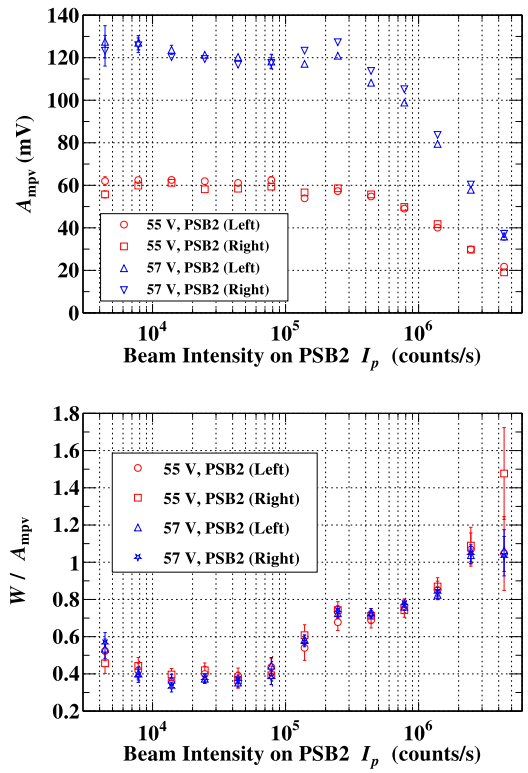

Fig. 10. The beam intensity I_p dependence of the most probable value of the signal amplitude A_{mpv} (top) and the FWHM W (bottom). FWHM W is normalized by A_{mpv}.

voltage by about ±2 V per MPPC at intensity > 100 kHz. The amplitude reduction and relative width broadening are considered to be partly due to the slow response of the bias-voltage power supply and the low-pass filter in the bias-voltage supply component of the amplifier in Fig. 2 of Ref. [1].

For a better understanding of the behavior in high rate conditions, we constructed a test bench to study in detail the high intensity conditions using LEDs irradiating the MPPCs. We achieved better stability of the A_{mpv} and W by using a different high-voltage power supply of the MPPCs (KIKUSUI PMX250-0.25 A) and by replacing the three 1.2 kOhm resistances in series in Fig. 2 of Ref. [1] with a 75 Ohm one. Therefore, we suspect that the deterioration at a high counting rate during data taking was partly due to the slow response of the bias-voltage power supply at a high intensity and the voltage drop in the resistors in the power-supply part of the amplifier circuit. These problems can be resolved by using a faster-response power supply and smaller resistances in the amplifier as partly confirmed in the test bench.

4. Conclusion

We systematically investigated the performance of the plastic scintillation counter with multiple MPPCs readout by irradiating it with 2.5 GeV/c proton beams. The time resolution and the amplitude stability were studied under the various configurations such as hit position, incident angle of the proton beams, number of MPPCs per end, bias voltages and beam intensity.

We found that the counter has a time resolution ranging between 55 and 80 ps for x_p in a range of ±24 cm and V_{bias}/N_{MPPC} = 55–58 V using 3 MPPCs at both ends. The time resolution of the counter becomes better as increasing the number of MPPC, the applied bias voltage or incident angle.

The performance of the counter fulfills our requirement up to 1 MHz. Beyond 1 MHz, we observed severe degradation of the time resolution. We also found that the amplitude starts to gradually decrease at a counting rate higher than 300 kHz and reaches 70% reduction at 4 MHz. We found possible reasons for the performance degradation and partly resolved the problem with further study.

The newly developed counter will be employed for one of the detectors in the WASA detector system [8]. We confirmed that the performance of the new counter satisfies the requirements of the planned experiments.

CRediT authorship contribution statement

R. Sekiya: Conceptualization, Formal analysis, Investigation, Writing – original draft, Writing – review & editing, Visualization. **V. Drozd:** Conceptualization, Formal analysis, Investigation, Writing – review & editing. **Y.K. Tanaka:** Conceptualization, Formal analysis, Investigation, Writing – original draft, Writing – review & editing, Supervision. **K. Itahashi:** Conceptualization, Formal analysis, Investigation, Writing – original draft, Writing – review & editing, Supervision. **H. Fujioka:** Conceptualization, Writing – review & editing. **S.Y. Matsumoto:** Conceptualization, Formal analysis, Writing – review & editing. **T.R. Saito:** Conceptualization, Writing – review & editing. **K. Suzuki:** Conceptualization, Writing – review & editing.

Declaration of competing interest

The authors declare that they have no known competing financial interests or personal relationships that could have appeared to influence the work reported in this paper.

Acknowledgments

We would like to thank the staffs of GSI and Institut für Kernphysik, Forschungszentrum Jülich and PANDA STT group for their cooperation during the beam time at COSY. This work is partly supported by JSPS Grants-in-Aid for Scientific Research (B) (Grant No. JP18H01242) and for Early-Career Scientists (Grant No. JP20K14499) and JSPS Fostering Joint International Research (B) (Grant No. JP20KK0070).

References

[1] P.W. Cattaneo, et al., Development of high precision timing counter based on plastic scintillator with SiPM readout, IEEE Trans. Nucl. Sci. 61 (5) (2014) 2657–2666, http://dx.doi.org/10.1109/TNS.2014.2347576.

[2] P.W. Cattaneo, et al., Time resolution of time-of-flight detector based on multiple scintillation counters readout by SiPMs, Nucl. Instrum. Methods Phys. Res. A 828 (2016) 191–200, http://dx.doi.org/10.1016/j.nima.2016.05.038.

[3] A. Stoykov, R. Scheuermann, K. Sedlak, A time resolution study with a plastic scintillator read out by a geiger-mode avalanche photodiode, Nucl. Instrum. Methods Phys. Res. A 695 (2012) 202–205, http://dx.doi.org/10.1016/j.nima.2011.11.011.

[4] M. Nishimura, et al., Full system of positron timing counter in MEG II having time resolution below 40 ps with fast plastic scintillator readout by SiPMs, Nucl. Instrum. Methods Phys. Res. A 958 (2020) 162785, http://dx.doi.org/10.1016/j.nima.2019.162785.

[5] A. Korzenev, et al., Plastic scintillator detector with the readout based on an array of large-area SiPMs for the ND280/T2K upgrade and SHiP experiments, in: Proceedings of the 5th International Workshop on New Photon-Detectors, PD18, https://journals.jps.jp/doi/abs/10.7566/JPSCP.27.011005.

[6] A. Alici, et al., Time resolution measurements with SiPMs coupled to a scintillator, J. Instrum. 13 (2018) P09012, http://dx.doi.org/10.1088/1748-0221/13/09/p09012.

[7] R. Onda, et al., Optimal design of plastic scintillator counter with multiple SiPM readouts for best time resolution, Nucl. Instrum. Methods, Phys. Res. A 936 (2019) 563–564, http://dx.doi.org/10.1016/j.nima.2018.10.070.

[8] H.-H. Adam, et al., Proposal for the wide angle shower apparatus (WASA) at COSY-Jülich WASA at COSY, 2004, https://arxiv.org/abs/nucl-ex/0411038.

[9] H. Geissel, et al., The GSI projectile fragment separator (FRS): a versatile magnetic system for relativistic heavy ions, Nucl. Instrum. Methods, Phys. Res. B 70 (1992) 286–297, http://dx.doi.org/10.1016/0168-583X(92)95944-M.

[10] Y.K. Tanaka, et al., Missing-mass spectroscopy of the $^{12}C(p,d)$ reaction near the η'-meson production threshold, Phys. Rev. C 97 (2018) 015202, https://link.aps.org/doi/10.1103/PhysRevC.97.015202.

[11] T.R. Saito, et al., New directions in hypernuclear physics, Nat. Rev. Phys. (2021) http://dx.doi.org/10.1038/s42254-021-00371-w.
[12] Hamamatsu Photonics, MPPC S13360 Series, https://www.hamamatsu.com/resources/pdf/ssd/s13360_series_kapd1052e.pdf.
[13] J. Hoffmann, et al., Programmable trigger processing module, VUPROM, in: Scientific Report 2007. GSI, Darmstadt, Jul. 2008, p. 256, https://citeseerx.ist.psu.edu/viewdoc/download?doi=10.1.1.162.1401&rep=rep1&type=pdf.
[14] A. Codino, The pulse digitization for measuring the time of flight of ionizing particles, Nucl. Instrum. Methods, Phys. Res. A 440 (2000) 199–201, http://dx.doi.org/10.1016/S0168-9002(99)00813-X.
[15] D.C.S. White, W.J. McDonald, Recent developments in subnanosecond timing with coaxial Ge(Li) detectors, Nucl. Instrum. Methods 115 (1974) 1–11, http://dx.doi.org/10.1016/0029-554X(74)90419-4.